character of the angular dependence of the luminescence intensity changes. The photographs show a section of the spectrum in which the direction of the luminescence radiation is bounded from above by a critical value of the angle ϕ, whose magnitude depends on the wavelength. The generation occurs at those wavelengths for which the direction of the critical angle coincides with the resonator axis. Since the critical angle depends strongly on the refractive index of the liquid, a change of several degrees in the temperature of the solution makes it possible to tune the radiation frequency over the entire luminescence band.

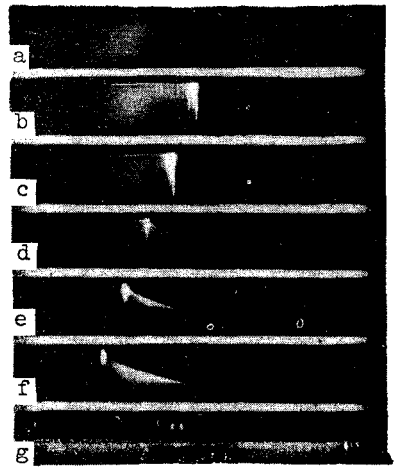

Fig. 2. Generation spectra at different temperatures: a - 13°C, b - 14°C, c - 15°C, d - 16°C, e - 17°C, f - 18°C, g - mercury-lamp spectrum.

3. In the absence of resonator mirrors we observed instead of generation a directional superluminescence with a broad spectrum. The divergence of the superluminescence radiation with respect to the angle ϕ was approximately 10^{-2} rad, indicating a strong dependence of the gain on the value of this angle. With respect to the azimuthal angle, on the other hand, the change of the intensity was small, so that the radiation was limited to the surface of a cone with a vertex angle 2ϕ. This is observed particularly clearly when the prism is replaced by a glass hemisphere and a pumping-light beam of round cross section is employed. In this case the anisotropy of the distribution of the superluminescence radiation over the azimuthal angle is determined only by the polarization of the pump radiation.

When the temperature is varied, the direction of the superluminescence radiation follows the variation of the critical angle for the internal-reflection boundary.

When the temperature was properly chosen, we were able to obtain generation in a resonator in which the mirrors are the end faces of the prism. This means that the reflection coefficient on the boundary between the glass and the solution reached in this case a value $R > 25$.

We consider the use of internal reflection advantageous primarily when the active medium is a thin layer, as is the case, for example, in semiconductor lasers.

PICOSECOND STRUCTURE OF THE EMISSION OF A LASER WITH A NONLINEAR ABSORBER

S.D. Fanchenko and B.A. Frolov
Submitted 26 June 1972
ZhETF Pis. Red. 16, No. 3, 147 - 150 (5 August 1972)

It is known [1, 2] that measurement of the duration of neodymium laser pulses in the mode-locking regime by the method of two-photon luminescence yields a scatter amounting to approximately one order of magnitude. In view of the ambiguity in the interpretation of the results of correlation two-photon measurements, a detailed study of the picosecond structure of the laser emission by this method is quite difficult. Direct observations of the time structure of the radiation [3, 4] had so far a time resolution not better than $(0.5 - 2) \times 10^{-11}$ sec. In the present study we used a "picochron" electron-optical image converter with a time resolution 5×10^{-13} sec for a direct

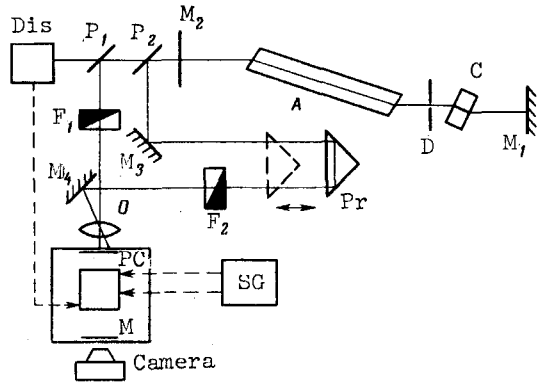

Fig. 1

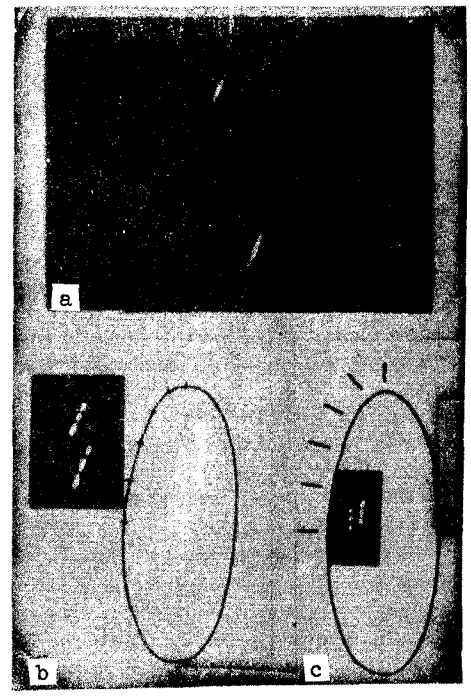

Fig. 2

Fig. 1. Diagram of neodymium-glass laser with Fabry-Perot resonator. Dis - laser-ignited discharge gap triggering the linear sweep of the picochron; SG - continuous sweep generator for the picochron image at wavelength 3 cm; PC - input photocathode of the picochron.

Fig. 2. Image converter pictures of the laser radiation. To indicate the scale, the trajectories of the elliptic sweep of the image are shown for the two observation channels. One division equals 5×10^{-12} sec.

observation of the time dependence of the radiation intensity of a neodymium laser.

The experimental setup is shown in Fig. 1. The laser resonator was made up of dielectric mirrors M_1 and M_2 deposited on wedge-like substrates. Neodymium-glass rod A of length 300 mm, and cell C with a solution of a nonlinear absorber (dye 3955) were mounted at the Brewster angle. Diaphragm D of 1 mm diameter was used for selection of the transverse modes.

The laser radiation could be investigated simultaneously along two channels with the aid of a system of beam-splitting plates and mirrors (P_2, P_1 and P_2, M_3, Pr, M_4 in Fig. 1). Displacement of the prism Pr made it possible to regulate the optical delay of the pulse in the second channel relative to the first.

A trochoidal image sweep with total duration 1.5×10^{-8} sec and a time resolution $\Delta\tau = 5 \times 10^{-13}$ sec was used in the picochron.

We obtained the following experimental results. Within a time 8×10^{-9} sec, corresponding to the axial period, there are observed one or several radiation pulses of duration $10^{-10} - 10^{-11}$ sec, just as in [3, 5]. Figure 2a shows an example of the time sweep of a single radiation pulse in the axial period, when observed along both channels. The good reproducibility of the results in both

channels made it possible to determine reliably the duration of this pulse.

The pulses were observed to have a temporal fine structure, the appearance of which was noted both in pulses with total duration 10^{-11} sec, and in much longer pulses.

Photometry of the image converter data with the use of a computer has enabled us to calculate for laser pulses with total duration on the order of 10^{-10} sec the autocorrelation functions, where a modulation was noticeable with a characteristic time 2.5×10^{-12} sec at a correlation length of approximately 1×10^{-11} sec.

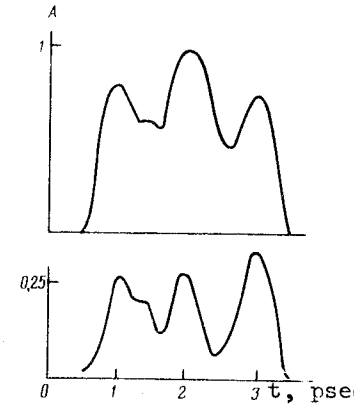

Fig. 3. Photometry curves of the pictures of Fig. 2c. Abscissas - time in picoseconds, ordinates - light flux in relative units.

Characteristic examples of the temporal fine structure of the laser radiation are shown in Figs. 2b and 2c. The observation was carried out simultaneously through both channels. In the case of Fig. 2b, a series of three spikes is observed in both channels, with total duration of approximately 3×10^{-12} sec. In the case of 2b, the series consists of four spikes and has a total duration of about 8×10^{-12} sec. The relative time shift of the channels was quite different in the cases of Figs. 2b and 2c. In the case of Fig. 2c, the maxima of the signal in one channel lie opposite the minima in the other. In the case of Fig. 2b, the relative shift of the channels is approximately 7×10^{-12} sec. Figure 3 shows the results of the photometry of the image-converter pictures in both observation channels for the case of Fig. 2c. Attention is called to the fact that the intervals between the maxima are the same on both photometry curves, within $\sim 10^{-13}$ sec, although the intensities of the registered signals differ: in the former case there are $N \approx 10$ photoelectrons in the input stage per resolved element in space and time, and in the latter case $N \approx 50$. The most probable distance between maxima was 2.5×10^{-12} sec.

Discussion and conclusions. It was observed experimentally that the minimum total duration of a single laser pulse in the axial period amounts to not less than $(8 - 10) \times 10^{-12}$ sec. The emission pulses with total duration $(10 - 100) \times 10^{-12}$ sec had a fine structure consisting of a series of three or four emission spikes with characteristic duration $(1 - 3) \times 10^{-12}$ sec.

The picosecond structure of the pulses was observed at picochron input-stage loads corresponding to emission of $N \sim 10^1 - 10^2$ photoelectrons from the resolved element of the input photocathode within the resolved time. In spite of the appearance of fluctuations that decrease the accuracy with which the absolute values of the signals are determined at small N, the relative positions of the maxima could be established with accuracy $\sim 10^{-13}$ sec, regardless of the delay time between the observation channels and regardless of the value of N. At $N > 10^3$ photoelectrons, no picosecond structure was observed, a fact that can be attributed to overloading of the input channel of the electron-optical converter.

In conclusion, the authors are grateful to E.K. Zavoiskii for valuable discussions and to S.D. Kaitmazov and P.G. Kryukov for consultations on laser problems.

[1] A.J. DeMaria, Electronics 41, 19 (1968).
[2] V.I. Malyshev, A.A. Sychev, and V.A. Babenko, ZhETF Pis. Red. 13, 592 (1970) [JETP Lett. 13, 422 (1970)].

[3] A.A. Malyutin and M.Ya. Shchelev, ibid. 9, 445 (1969) [9, 266 (1969)].
[4] D.J. Bradley, B. Liddy, and W.E. Sleat, Opt. Commun. 2, 391 (1971).
[5] R. Harrach and C. Kachen, J. Appl. Phys. 39, 2482 (1968).

CONCERNING THE MEASUREMENT OF THE MAGNETIC MOMENT OF THE Λ^0 HYPERON

L.M. Barkov, I.I. Gurevich, L.A. Makar'ina, V.P. Martem'yanov, A.P. Mishakova, V.V. Ogurtsov, L.V. Surkova, V.G. Tarasenkov, A.I. Fesenko, S.Kh. Khakimov, L.A. Chernysheva, and S.A. Chueva
Submitted 28 June 1972
ZhETF Pis. Red. 16, No. 3, 151 - 153 (5 August 1972)

In [1], the authors of the present article described an experiment on the measurement of the magnetic moment of the Λ^0 hyperon and presented the preliminary experimental results. In this experiment, the magnetic moment of the hyperon was determined from the angle of rotation of the hyperon spin in a strong plused magnetic field of 220 kG intensity. The polarized hyperons were produced in a polyethylene target in the reaction $\pi^+ + p \to \Lambda^0 + K^0$ at an incident π^--meson momentum 1.07 GeV/c. The hyperons produced in the polyethylene target traveled in a strong longitudinal magnetic field and decayed on reaching the emulsion stack. The initial position of the hyperon spin was determined from the direction of the polarization vector at production, and the final position was determined from the angular distribution of the π^- mesons of the $\Lambda^0 \to p + \pi^-$ decay. Owing to violation of spatial parity in Λ^0 decay, this angular distribution is given by

$$f(\Theta) = \frac{1 + \alpha P \cos\Theta}{2},$$

where Θ is the c.m.s. angle between the direction of the polarization vector at the instant of decay and the momentum of the decay π^- meson, α is the asymmetry coefficient, and P is the degree of polarization of the hyperons.

Different variants of experiments on the measurement of the magnetic moment of the Λ^0 hyperon were realized in [1 - 7]. As a rule these are laborious experiments that require the efforts of a large staff for many years.

The accuracy with which the magnetic moment of the Λ^0 hyperon is determined is $\Delta\mu \sim (1/H_{av}\ell\sqrt{N})$, where H_{av} is the average value of the magnetic field along the flight trajectory, ℓ is the flight distance, and N is the number of decays recorded in the track detector. In the authors' opinion the use of magnetic fields of high intensity is the most promising from the point of view of decreasing the error in the determination of the magnetic moments of the hyperons. Whereas a few yeara ago this meant magnetic fields of several hundred kilogause, now, following a 1971 study by the CERN group [7], in which the accuracy of determination of the magnetic moment of the Λ^0 hyperon was greatly increased, one should speak of megagauss fields. This pertains primarily to experiments in which the track detector is a nuclear emulsion, for which there is no automatic processing method. In experiments in which spark and bubble chambers are used as detectors, a direct increase of the statistics when working with magnetic fields $\sim$100 kG can still give a higher accuracy within a conceivable time of 2 - 3 years.

The reduction of the entire material obtained in our study [1] would require a few more years. The accuracy with which the magnetic moment of the Λ^0 hyperon was measured would then be comparable with but not higher than the accuracy of [7]. The authors have therefore deemed it advisable to terminate the experiments in magnetic fields of 220 kG and report the final result.